Available online at www.sciencedirect.com
ScienceDirect
C. R. Physique 10 (2009) 207–215
COMPTES RENDUS PHYSIQUE

Laser acceleration of particles in plasmas / Accélération laser de particules dans les plasmas

Theory and simulation of ion acceleration with circularly polarized laser pulses

Andrea Macchi [a,b,*], Tatiana V. Liseikina [c,1], Sara Tuveri [b], Silvia Veghini [b]

[a] *CNR/INFM/polyLAB, 56127 Pisa, Italy*
[b] *Department of Physics "E. Fermi", University of Pisa, Largo B. Pontecorvo 3, 56127 Pisa, Italy*
[c] *Max Planck Institute for Nuclear Physics, 69029 Heidelberg, Germany*

Available online 29 April 2009

Abstract

Ion acceleration driven by the radiation pressure of circularly polarized pulses is investigated via analytical modeling and particle-in-cell simulations. Both thick and thin targets, i.e. the "hole boring" and "light sail" regimes are considered. Parametric studies in one spatial dimension are used to determine the optimal thickness of thin targets and to address the effects of preformed plasma profiles and laser pulse ellipticity in thick targets. Three-dimensional (3D) simulations show that "flat-top" radial profiles of the intensity are required to prevent early laser pulse breakthrough in thin targets. The 3D simulations are also used to address the issue of the conservation of the angular momentum of the laser pulse and its absorption in the plasma. ***To cite this article: A. Macchi et al., C. R. Physique 10 (2009).***

Résumé

Théorie et simulation de l'accélération des ions par impulsions laser à polarisation circulaire. L'accélération des ions par la pression de radiation des impulsions laser avec polarisation circulaire a été étudiée à l'aide de modèles analytiques et de simulations "*particle-in-cell*". Les deux régimes de cibles épaisses et minces, c'est-à-dire de "*hole boring*" et "*light sail*" ont été considérés. Des études paramétriques dans une dimension spatiale ont été réalisées afin de déterminer l'épaisseur optimale des cibles minces et pour étudier l'effet des profils de densité plasma préformés et l'effet de l'ellipticité de l'impulsion dans cibles épaisses. Les simulations tridimensionnelles (3D) montrent que des impulsions avec des profils radiaux plats en intensité sont nécessaires pour prévenir la pénétration de l'impulsion à travers la cible. Les simulations 3D ont aussi été utilisées pour étudier la conservation du moment angulaire de l'impulsion laser et son absorption dans le plasma. ***Pour citer cet article : A. Macchi et al., C. R. Physique 10 (2009).***

Keywords: Laser–plasma acceleration; Ion acceleration; Radiation pressure; Circular polarization

Mots-clés : Accéleration laser–plasma ; Accélération des ions ; Pression de radiation ; Polarisation circulaire

* Corresponding author at: Department of Physics "E. Fermi", University of Pisa, Largo B. Pontecorvo 3, 56127 Pisa, Italy.
E-mail address: macchi@df.unipi.it (A. Macchi).
URL: http://www.df.unipi.it/~macchi (A. Macchi).
[1] On leave from Institute of Computational Technologies, SD-RAS, Novosibirsk, Russia.

1631-0705/$ – see front matter
doi:10.1016/j.crhy.2009.03.002

1. Introduction

Radiation Pressure Acceleration (RPA) is a possible route to the acceleration of ions up to energies in the relativistic domain (GeV/nucleon), alternative to the Target Normal Sheath Acceleration (TNSA) mechanism which explains ion acceleration from thin solid targets in present-day experiments (see [1] for a review). The interest in RPA was stimulated by Particle-In-Cell (PIC) simulations of Esirkepov et al. [2,3] showing that at intensities $I > 5 \times 10^{21}$ W cm^{-2} RPA starts to dominate over TNSA, and that at $I \gtrsim 10^{23}$ W cm^{-2} and using a thin foil target, an efficient generation of GeV ions and a linear scaling of ion energy vs. the pulse energy may be obtained. These characteristic features of RPA, very appealing for foreseen applications of ion acceleration, may be qualitatively understood using the simple model of a perfectly reflecting mirror accelerated by a normally incident plane wave. Due to the Doppler effect, the frequency ω of each incoming photon reflected by the mirror moving at the velocity $V = \beta c$ in the laboratory frame is downshifted to ω' according to the relation $\omega' = \omega(1-\beta)/(1+\beta)$, so that almost all of the energy $\hbar\omega$ of the photon is delivered to the target in the limit $\beta \to 1$ and, since the number of photons is conserved for a perfect mirror, a complete conversion of the wave energy into mechanical energy is obtained.

Intensities exceeding 10^{23} W cm^{-2} are not available yet, but a dominance of RPA over TNSA may be already obtained at much lower intensity if a laser pulse with circular polarization (CP), instead of linear polarization (LP), is used. In fact, in such conditions the acceleration of "fast" electrons at the laser–plasma interface is almost suppressed, ruling out TNSA which is driven from the space charge produced by energetic electrons escaping in vacuum. The suppression of fast electrons for CP can be understood by noting that models of electron acceleration at a sharp plasma surface ([4,5] and references therein) require the driving force to have an *oscillating* component along the density gradient. For normal incidence, such component is given by the $\mathbf{J} \times \mathbf{B}$ term at 2ω (with experimental evidence given by Ref. [6]) which however vanishes for CP (see Section 2 for a discussion based on a simple model).

Radiation Pressure Acceleration using Circular Polarization (CP-RPA) was first studied by our group [7,8] by considering "thick" targets, such that during the laser pulse only a finite layer of the target at its front surface is accelerated, forming a dense bunch of ions (neutralized by "cold" electrons) entering the target. Dramatic differences in ion acceleration were observed between CP and LP [7,8]. Later, three groups [9–12] studied the acceleration of "thin" foils, such that the whole target is accelerated. In this regime, the use of CP is particularly important to prevent the foil expansion due to the "thermal" pressure of electrons, allowing the acceleration of the target as a single "rigid" object and preserving the inherent monoenergeticity after the acceleration stage. In good accordance with the predictions of the "mirror" model, it was found that sub-micrometric targets may be accelerated up to energies corresponding to GeV/nucleon using petawatt pulses with picosecond duration, which are feasible with current technology. This perspective has stimulated additional theoretical and numerical investigations [13–16].

In this article, we review our analytical and simulation work [7,8,17,18] on both the "thick" and "thin" regimes of CP-RPA which are also named "hole boring" (HB) and "light sail" (LS) regimes, respectively. Most recent work from our group included a) a study of the "optimal" target thickness in the LS case, b) a preliminary evaluation of "preplasma" effects, and c) three-dimensional (3D) simulations of CP-RPA to address in particular the issue of the absorption of the angular momentum of the laser pulse by the plasma.

2. The role of the pulse polarization: a simple model

A simple and possibly pedagogical "minimal" model to show the role of the polarization in laser interaction with an overdense plasma at normal incidence may be described as follows. We assume a plane, elliptically polarized wave of frequency ω incident on an overdense plasma with a step-like profile of the electron density $n_e(x) = n_0\Theta(x)$, and $\omega_p > \omega$ being $\omega_p = \sqrt{4\pi n_0 e^2/m_e}$ the plasma frequency. For sufficiently low intensity (neglecting relativistic and strong charge separation effects) the vector potential inside the plasma has the form

$$\mathbf{A}(x,t) = \frac{A(0)}{\sqrt{1+\epsilon^2}} \mathrm{e}^{-x/d_p} (\hat{y}\cos\omega t + \epsilon\hat{z}\cos\omega t) \tag{1}$$

where $d_p = c/\sqrt{\omega_p^2 - \omega^2}$ and ϵ is the ellipticity ($0 < \epsilon < 1$). The longitudinal force on electrons due to the $\mathbf{v} \times \mathbf{B}$ term is then obtained as

$$F_x = -\frac{e^2}{2m_e c^2}\partial_x \mathbf{A}^2 = F_0 \mathrm{e}^{-2x/d_p}\left(1 + \frac{1-\epsilon^2}{1+\epsilon^2}\cos 2\omega t\right) \tag{2}$$

where $F_0 = (e^2 A(0)^2/2 d_p m_e c^2)$. By solving the equations of the longitudinal motion of electrons for the secular and 2ω components we obtain the electric field and the electron density perturbation

$$E_x = \frac{F_0}{e} \mathrm{e}^{-2x/d_p} \left(1 + \frac{1-\epsilon^2}{1+\epsilon^2} \frac{\cos 2\omega t}{1 - 4\omega^2/\omega_p^2} \right), \quad \delta n_e = -\frac{1}{4\pi e} \partial_x E_x \tag{3}$$

The denominator in the oscillating term of E_x arises from the resonant excitation of plasma oscillations when $2\omega = \omega_p$. For LP ($\epsilon = 0$), the peak amplitude of the oscillating term is larger than the secular term, and as a consequence some electrons are dragged into the vacuum side, as can be evidenced by calculating the quantity

$$\Delta N_e(t) = \int_0^{+\infty} \delta n_e \, \mathrm{d}x = \frac{F_0}{4\pi e^2} \left(1 + \frac{1-\epsilon^2}{1+\epsilon^2} \frac{\cos 2\omega t}{1 - 4\omega^2/\omega_p^2} \right) \tag{4}$$

When $\Delta N_e(t) > 0$, electrons are piling up inside the plasma and a positive surface charge appears to ensure quasineutrality. However, if the oscillating term becomes larger than the secular one (and this always happens if $\epsilon = 0$, i.e. for LP), $\Delta N_e(t) < 0$ occurs implying that some electrons cross the $x = 0$ surface entering the vacuum side. In this case a regular, periodic solution does not exist anymore. This is a signature of the onset of self-intersection of electron trajectories in vacuum leading to heating and appearance of fast electron "jets" twice per laser cycle. For CP ($\epsilon = 1$), however, the oscillating terms vanish, the electric force on electrons balances the ponderomotive force ($F_x - eE_x = 0$) and no electron heating occurs. The model suggests an ellipticity threshold $\epsilon_T = (\omega_p^2/2\omega^2 - 1)^{-1/2}$ such that for $\epsilon > \epsilon_T$ we have $\Delta N_e(t) > 0$ at any t, and "vacuum heating" should be inhibited.

These conclusions can be verified to hold also at higher intensity with numerical methods. For example, a PIC simulation with fixed ions and a CP, semi-infinite laser pulse with a sufficiently slow rising edge shows that the equilibrium profiles of E_x and δn_e are in excellent agreement with an exact analytical solution including relativistic and strong charge separation effects [19,20].

3. Thick targets: density breaking and ion bunch generation

The electrostatic field E_x created by the electron displacement accelerates ions modifying the density profile. A self-consistent, time-dependent solution of the wave penetration is not available. In Ref. [7] a phenomenological model giving simple analytical solutions and accounting for the most prominent features observed in simulations for the "thick" target or "hole boring" regime was obtained by taking an "ad hoc" spatial and temporal profile of the ponderomotive force F_x and assuming the quasi-equilibrium condition for electrons to hold as the ions move. A brief description of the model is given in Fig. 1 and its caption.

The equations of motion are valid until the time τ_b at which all the ions initially located in the layer of electron compression ($x_d < x < x_s$ in Fig. 1) reach the point $x = x_s$; here, the ion density becomes singular and the fastest ions overcome the slowest ones so that hydrodynamical or "wave" breaking for the ion fluid occurs. At the time t_i, the maximum ion velocity and the corresponding energy for a laser pulse of constant intensity are given by

$$\frac{v_{im}}{c} = 2\sqrt{\frac{Z}{A}\frac{m_e}{m_p}\frac{n_c}{n_e}} a_L, \quad \mathcal{E}_m = \frac{1}{2} m_i v_{im}^2 = 2Z m_e c^2 \frac{n_c}{n_e} a_L^2 \tag{5}$$

where $a_L = 0.85(I\lambda^2/10^{18}\ \mathrm{W\,\mu m^2/cm^2})^{1/2}$ is the laser amplitude in dimensionless units. These formulas are valid for non-relativistic ion velocities; relativistic corrections are considered in Ref. [16].

The details of the ion spectrum depend on the highly transient stage of wave breaking and may be studied mostly via simulations. Fig. 1b) shows three snapshots from a 1D PIC simulation, showing the generation of the electrostatic field, the very strong spiking of the ion density at the instant of wave breaking and the formation of a short-duration, high-density "bunch" moving in the forward direction at velocity $\simeq v_{im}$. The heating of electrons is significant only around the "breaking" event and the electron energies are lower by nearly two order of magnitudes than the value observed for LP interaction at the same intensity [7,8]. A detailed study of the dynamics of wave breaking in a very similar context has been reported in Ref. [21].

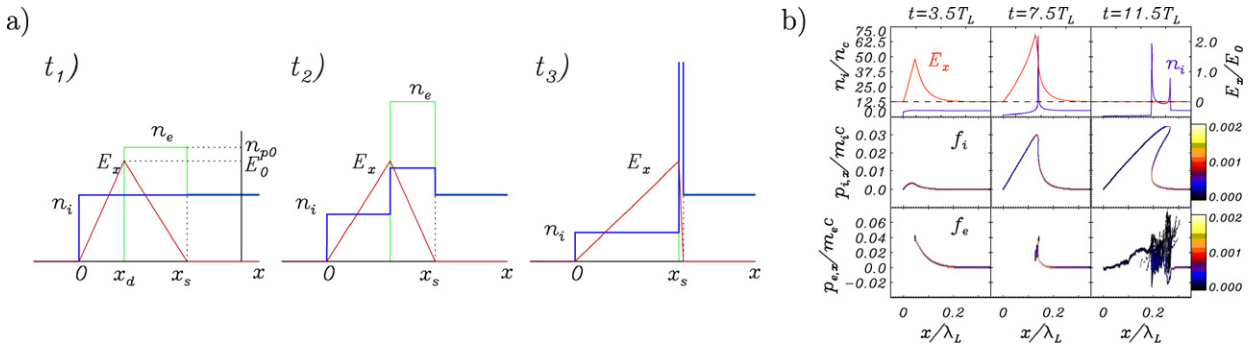

Fig. 1. a): model for RPA of ions at the front target surface [7,17]. The plots show the spatial profiles of E_x (red), n_i (blue) and n_e (green) at three different times. The ponderomotive force $F_x = eE_x$ in the region where $n_e \neq 0$. Due to conservation laws, model parameters are related by $E_0 = 4\pi e n_0 x_d$, $n_0 x_s = n_{p0}(x_s - x_d)$, and $E_0 e n_{p0}(x_s - x_d)/2 \simeq 2I/c$ where $x_s - x_d \simeq c/2\omega_p$. At the time t_1, ions have not moved yet and electrons have been pushed creating the charge separation field; at t_2, E_x accelerates ions and pile them up in the evanescence region, while electrons rearrange themselves to keep the force balance condition; at t_3, the density peaks up to infinite values since all ions starting from the $x_d < x < x_s$ get to the point $x = x_s$ at the same time, and "wave breaking" occurs. b): 1D PIC simulation of the interaction of a short CP laser pulse with an overdense, step-boundary plasma [17]. The figure shows n_i and E_x (top row) and the (x, p_x) phase space distribution for ions (f_i, middle row) and electrons (f_e, bottom row) at different times in units of the laser period T_L. The laser pulse has peak amplitude $a = 2$ and duration $\tau = 6T_L$ (FWHM). The initial density is $n_0 = 5n_c$ where n_c is the cut-off density. The x coordinate is normalized to λ, the density to n_c, the electric field to $m_e\omega c/e$ and the momenta to $m_e c$ and $m_i c$, respectively.

Some further insight into the dynamics of ion bunch formation is obtained by looking at simulations with *elliptical* polarization for different values of the ellipticity ϵ, since this allows to vary the relative importance of secular and oscillating components in the accelerating fields. They are also of interest to test the sensitivity of the RPA regime to values of $\epsilon < 1$ as it may occur in experiments. The snapshots shown in Fig. 2 for simulations having the same plasma target and a laser pulse of fixed energy and duration but different values of ϵ show the tendency to the formation of multiple ion "bunches". This effect may be explained by noting that, due to the oscillating component in E_x, ions now cross the evanescence point at different times corresponding to positive maxima of E_x. The phase space for $\epsilon = 0.5$ shows the "X"-type structure whose origin has been discussed in Ref. [21]. The electron heating is observed to increase as ϵ decreases from 1 (CP) to 0 (LP). Very recently a similar study has been reported in Ref. [22], showing a "threshold" value for ϵ which depends weakly on the laser intensity. This is in qualitative agreement with our simple model (Section 2) where the intensity dependence may arise in the resonant denominator due to the relativistic correction to the plasma frequency $\omega_p^2 \to \omega_p^2/\sqrt{1+a^2}$.

Parametric 1D runs were also performed to study the effect of a "preplasma", i.e. a density profile smoother than a step-like one, which could be typically produced in experiments by a prepulse preceding the ultrashort, superintense pulse. Such study is also of interest because the scaling laws (5) predict the ion energy to be inversely proportional to the density. Although these relations have been obtained for a step-like profile, they suggest that in a preplasma the interaction occurs near the $n_e \simeq n_c$ layer leading to higher ion energies. This effect was confirmed in the preliminary simulations shown in Ref. [18], which show that ion bunch formation occurs also in a preplasma, suggesting the possible use of prepulse control to achieve higher energies. The dependence of ion energy and conversion efficiency (defined as the ratio of the total energy of the ions over the energy of the laser pulse) on the density scalelength $L = n_c/|\partial_x n_0|_{n_0=n_c}$ for a given laser pulse are shown in Fig. 2b).

In general, because of the large value of n_e/n_c ($\sim 10^2$) for solid densities and the typical laser wavelength ~ 1 μm, any possibility (e.g., by special target materials) to achieve a laser–plasma interaction at smaller values of n_c/n_e would be important to obtain high ion energies in the "hole boring" regime. We note that, usually, 2D and in particular 3D simulations are performed for relatively small values of n_e/n_c because of computational limitations, since the need to resolve length scales smaller than $c/\omega_p \sim 1/\sqrt{n_e}$ and density regions where $n_e < n_c$ forces to use large numbers of small cells and large numbers of particles. At least, an estimate of the scaling of all relevant quantities such as ion energy and conversion efficiency with n_e is thus needed to extrapolate simulation results to feasible experimental parameters.

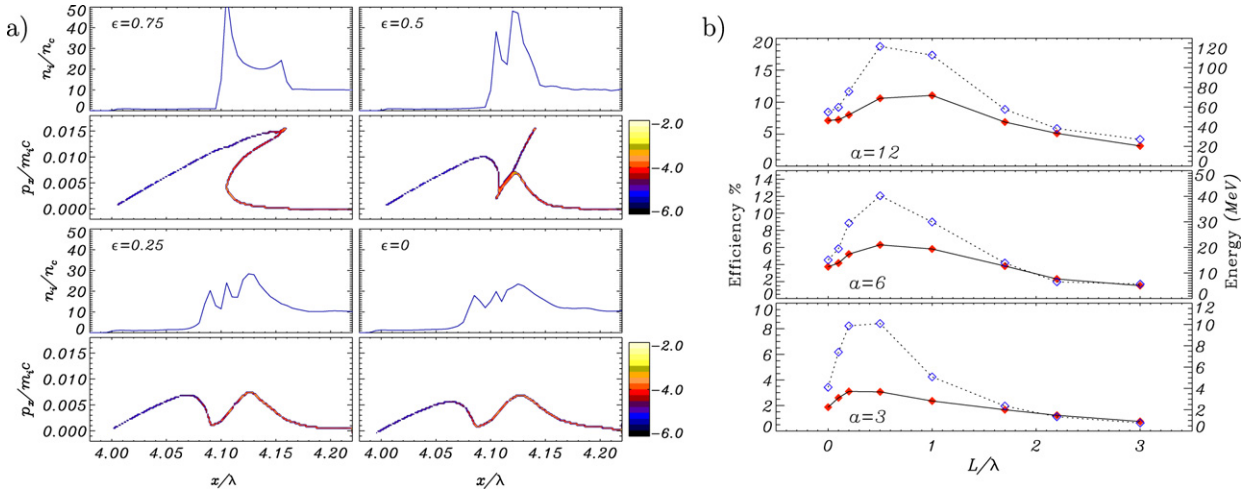

Fig. 2. Results from parametric 1D simulations. a): snapshots of n_i and $f_i(x, p_x)$ (in $\log_{10}$ scale) from simulations with different ellipticity ϵ. Common parameters to all runs are $n_0 = 10n_c$, $a = 2$, and $\tau = 12T_L$. b): interaction with preformed plasmas [18]. Conversion efficiency (red filled diamonds, solid line) and peak energy (blue empty diamonds, dashed line) of ions as a function of the density scalelength L in preplasma and the laser amplitude a. The density profile is described by a $\sim(x - x_0)^4$ function up to a peak density $n_0 = 16n_c$. The pulse duration $\tau = 9T_L$.

4. Thin targets: optimal thickness and heating effects

The analysis of the RPA dynamics for "thick" targets outlined above now allows us to define "thin" targets in this context. In thick targets, after wave breaking the fastest ions overturn the slowest ones, penetrate into the overdense plasma and are not accelerated anymore. To obtain high energies the laser pulse must be able to repeat the acceleration stage over the same ions. Thus, the target thickness must be close to the depth of the compression layer (the parameter $\ell_s = x_s - x_d$ in Fig. 1) in order for repeated or "cyclic" RPA to occur. If the solid target contains hydrogen ions, they will gain higher velocity in a first stage, but overturning other ions they will be screened by the laser pulse until heavier ions reach them. Thus, ions of different Z/A ratio will tend to ultimately be accelerated to the same velocity, so that RPA of thin foils appears to be most suitable for the acceleration or ions heavier than protons, e.g., carbon.

Although due to the above considerations the target may not be considered as a "rigid" object, the accelerating mirror or "light sail" model gives reasonable estimates for the target velocity $V = \beta c$ as a function of the laser pulse energy. The equations of motion are

$$\frac{\mathrm{d}(\gamma\beta)}{\mathrm{d}t} = \frac{2I(t - X/c)}{\rho d c^2}\frac{1-\beta}{1+\beta}R(\omega'), \qquad \frac{\mathrm{d}X}{\mathrm{d}t} = \beta c \tag{6}$$

where ρ and d are the mass density and thickness of the mirror and R is its reflectivity, which can be written as a function of the pulse frequency in the rest frame ω'. An analytical solution is found for $R = 1$ and constant intensity

$$\gamma\beta = \left[\sinh\psi(t) - \frac{1}{4\sinh\psi(t)}\right], \qquad \psi(t) = \frac{1}{3}\operatorname{arcsinh}\left(\frac{6It}{\rho d c^2} + 2\right) \tag{7}$$

Higher velocities and efficiency are expected for lighter targets, but as ρd decreases the target tends to become transparent to the laser light. One thus expect to find an "optimal" thickness d_{opt} to exist for a given laser intensity. Fig. 3a) shows a set of 1D parametric simulations in a range of presently accessible intensities (10^{19}–10^{21} W cm^{-2}). It is found that d_{opt} increases with pulse intensity (presumably due to induced relativistic transparency) and has typical values of $\approx 10^{-2}$ μm. Such ultrathin targets are technologically feasible but will require the complete suppression of prepulses in experiments.

We obtained an analytical solution for the motion of the mirror even in the case of partial reflectivity by using for the latter the model of a "delta-like" foil [23] and including the effects of self-induced transparency. The resulting energy per nucleon as a function of the target thickness and the pulse fluence (energy per unit surface) is shown in Fig. 3b). There is qualitative agreement with the numerical simulations although the model predicts lower ion energies.

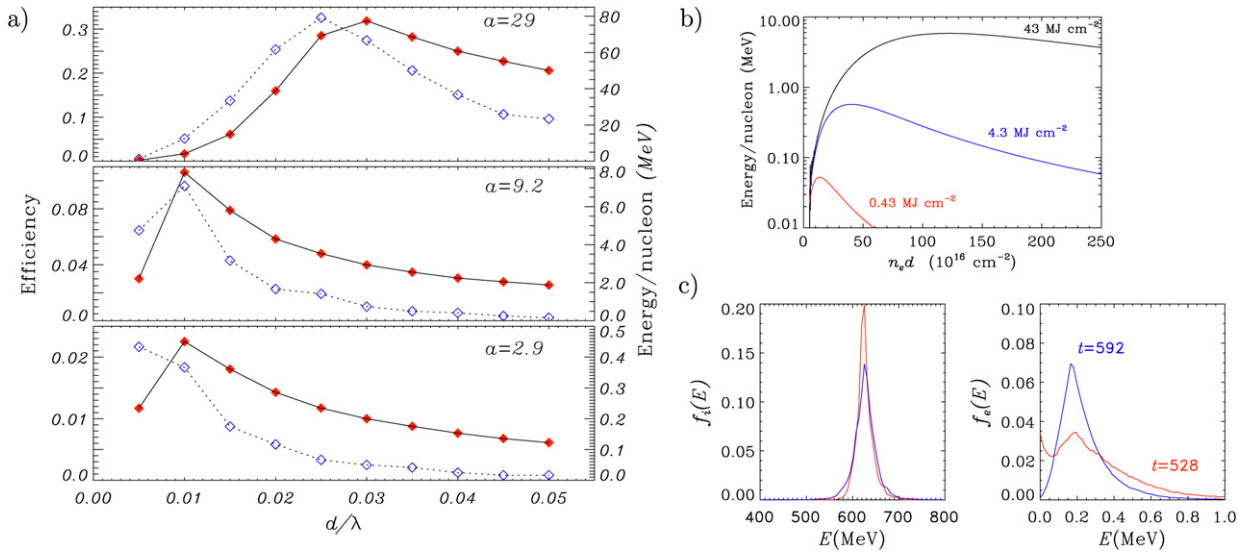

Fig. 3. a): energy conversion efficiency (red filled diamonds) and peak energy per nucleon (blue empty diamonds) as a function of the target thickness d and pulse amplitude a from 1D PIC simulations [18]. Common parameters to all runs are $\tau = 9T_L$, $n_e = 250n_c$ and $Z/A = 1/2$. b): analytical calculation of the energy per nucleon as a function of the areal density $n_e d$ of the target and of the pulse fluence. c): energy spectra of ions and electrons from a simulation of the interaction of a 400 fs, 1.8×10^{20} W cm^{-2} pulse with a 0.056 μm thick carbon target ($n_e = 250n_c$), for two different times (in fs).

A simple energy balance argument shows that to accelerate a solid target of "optimal" thickness $\approx 10^{-2}$ μm up to velocities corresponding to energies per nucleon ≈ 1 GeV, a pulse energy per unit surface $\approx 10^8$ J cm^{-2} is needed. The width of the energy spectrum is also an issue. The simulation results shown in Fig. 3c) show that a spectrum with $\simeq 5\%$ spread is obtained at the end of the laser pulse. However, some broadening of the energy spectrum is observed also after the acceleration stage. This seems to be related to a relatively abrupt increase of the absorption fraction into electrons near the end of the laser pulse, as the radiation pressure decreases. The resulting electron "temperature", although orders of magnitude lower than the quiver energy, may be sufficient to cause some expansion of the thin foil and to broaden the ion spectrum.

5. Multi-dimensional effects

The above analysis is based on 1D modeling and simulations, which for example do not account for effects related to the finite transverse size of the laser pulse. As an obvious consequence, the intensity distribution implies that the radiation pressure on the plasma is inhomogeneous, leading to a broader ion energy spectrum, with less energetic ions at the periphery of the laser spot. Moreover, a finite pulse waist of radius r_L implies longitudinal field components $E_\parallel \approx (\lambda/r_L)E_\perp$ at the edge of the spot, causing local heating of electrons. The bending of the plasma surface caused by hole boring or foil deformation also increases the electron heating because the local angle of incidence does not vanish anymore. However, 2D simulations [7,8,11,12] show that these effects do not cause a failure of the CP-RPA, and the differences with the LP case are still evident [8]. It has been shown that pulses with a "flat-top" (e.g., supergaussian) [11] intensity profile allow to preserve a narrow ion spectrum and a very low divergence (a few degrees).

The onset of surface instabilities, e.g. of density rippling, has also been studied by 2D simulations. A Rayleigh–Taylor-like instability driven by radiation pressure has been characterized in Ref. [24] for thin foils accelerated by LP pulses. However, the comparison of thick targets simulations for CP and LP show that the surface instability is weaker for CP [17]. This suggests that additional effects besides RPA contribute to the dynamics of the instability.

Since a CP wave carries a net angular momentum, conservation of the latter poses an additional constraint on the interaction. This gives a specific motivation for 3D simulations of CP-RPA. The issue of angular momentum absorption in the plasma has been studied in the past mostly for underdense plasmas and in close connection with the Inverse Faraday Effect, i.e. the generation of axial magnetic fields, and apparently it has often been a subject of controversy and misunderstanding (see e.g. [25,26] and references therein). In the present context it is noticeable

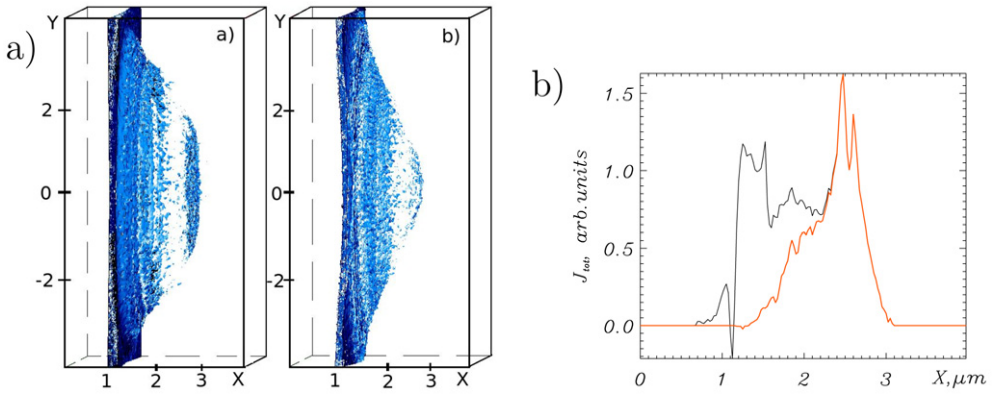

Fig. 4. Three-dimensional simulations of CP-RPA of a thin foil target. a): the ion density n_i at $t = 40T_L$ for two different radial profiles of the laser intensity, a supergaussian $\sim\exp(-r^4/r_s^4)$ or "flat-top" (left) and a Gaussian $\sim\exp(-r^2/r_g^2)$ (right) profile, with $r_s = 2.5\lambda$ and $r_g = 2.4\lambda$. Common simulation parameters are $n_0 = 16n_c$, $d = 0.4\lambda$, $a = 5$ and $\tau = 10T_L$. b): the azimuthal ion current $J_{i,\varphi}$ averaged over the transverse plane (y, z), t=130 fs versus longitudinal coordinate, showing the angular momentum absorption into ions [18]. The black and red lines correspond to an average over a circle with radius $r = 4.5\lambda$ and 2.5λ, respectively, around the x-axis.

that, according to the accelerating mirror model, absorption of angular momentum by the target may vanish even for nearly complete energy absorption. In fact, the photon "spin" is $\hbar$ and independent from the frequency, while in the reflection of a photon from the mirror the direction of the spin is not reversed (as it happens for the momentum), so that the conservation of photon number in any frame implies that no angular momentum is absorbed by the target at all. Thus, the amount of angular momentum absorbed during CP-RPA gives an indication of non-adiabatic or dissipative processes at play in the laser–plasma interaction.

Fig. 4a) shows a 3D snapshot of the ion density for two simulations having identical parameters but different radial profiles of the intensity, i.e. a Gaussian and a supergaussian "flat-top" profile. The thickness of the target was chosen to be close to the "optimal" value inferred from the 1D parametric study. However, for the Gaussian pulse case, the lateral expansion of the central region of the target causes an early breakthrough of the laser pulse through the plasma, with a detrimental effect on the ion acceleration. The use of a "flat-top" pulse prevents the breakthrough and leads to an ion beam with very low divergence and energy values close to those inferred from the 1D analysis.

The fraction A_L of the angular momentum of the pulse transferred to the plasma was evaluated directly from the phase space distribution of the particles and compared to the energy absorption A_E. It is found that $A_L \lesssim A_E$ showing that a substantial part of the energy is absorbed via non-adiabatic processes (i.e. violating the conservation of photon number). It is noticeable that the density of axial angular momentum of the incident pulse is given by $\ell_x = \ell_x(r) = -\frac{r}{2c\omega}\partial_r I(r)$, which peaks at the edge of the beam where the axial components of the oscillating electric field have their maximum, i.e. where most of the electron heating occurs. Thus, non-adiabatic heating of electrons at the edge of the beam is likely to provide a channel for angular momentum absorption. However, the simulations show that eventually, after the end of the laser pulse, most of the absorbed angular momentum is given to ions. The absorption of angular momentum should lead to a torque on the ions and to the appearance of a steady azimuthal current. Such a net current can be evidenced by an average over the transverse plane, as in Fig. 4b), as the actual distribution is rather complicated. No regular magnetic field is found on the axis, i.e. there is no significant Inverse Faraday Effect associated to CP-RPA.

6. Discussion

The "light sail" regime of CP-RPA is very attractive for the possibility to accelerate a large number of ions (presumably of carbon or heavier elements) to GeV energies. The scheme requires ultrathin targets and, consequently, laser pulses with extremely high contrast [27]. Our simulations show that, in addition, flat-top intensity profiles may be crucial to reach the highest energies as well as to achieve high collimation and a monoenergetic spectrum.

The thick target or "hole boring" regime allows one to reach much lower energies with present-day intensities and solid target densities. However, this regime requires less critical conditions than the "light sail", and may be useful for applications requiring high densities of ions with moderate energies (up to a few MeV). Moreover, our preliminary

study of RPA in preformed plasma profiles suggest that the scaling with density allows to obtain energies higher than the values expected for solid densities and same pulse parameters. It might be also of interest to investigate RPA with CO_2 pulses in gas jets, where the gas density can be tuned to be only slightly over n_c and, in addition, high repetition rates would be possible.

Presently, no experimental results on CP interaction at normal incidence (or in conditions significantly close to such "optimal" conditions) have been reported yet in publications, but devoted experiments are planned or have been proposed in several facilities. For interactions with linearly polarized pulses, radiation pressure effects have been claimed to play a dominant role in a few experiments for different conditions [28–30] as well as in several phenomena observed in simulations (e.g. "laser piston" [2], surface rippling [24] or "shock acceleration" [31]). The study of circularly polarized interactions, besides its potential for ion acceleration, may be very useful for a detailed understanding of radiation pressure effects as these latter can be separated from effects due to fast electrons.

Acknowledgements

We are grateful to M. Borghesi, F. Cattani, F. Cornolti and D. Prellino for their previous contributions on the topics of this paper and to many colleagues including D. Bauer, F. Ceccherini, T. Ceccotti, S. Kar, E. Lefebvre, F. Pegoraro, S. Propuzhenko, and M. Zepf, for useful discussions or suggestions. We thank I. Klonova for the French translation of the abstract. The 3D simulations were performed on the computing clusters at CINECA, Bologna (sponsored by the CNR/INFM supercomputing initiative) and at MPI-K, Heidelberg. Part of the work was performed during a stay of two of the authors at Queen's University, Belfast, supported by a Visiting Research Fellowship (A.M.) and by COST-P14 (S.T.). Support from CNR via a RSTL project is also acknowledged.

References

[1] M. Borghesi, J. Fuchs, S.V. Bulanov, A.J. MacKinnon, P.K. Patel, M. Roth, Fusion Sci. Technol. 49 (2006) 412.
[2] T. Esirkepov, M. Borghesi, S.V. Bulanov, G. Mourou, T. Tajima, Phys. Rev. Lett. 92 (2004) 175003.
[3] T. Esirkepov, M. Yamagiwa, T. Tajima, Phys. Rev. Lett. 96 (2006) 105001.
[4] P. Gibbon, Short Pulse Laser Interactions with Matter: An Introduction, Imperial College Press, London, 2005.
[5] D. Bauer, P. Mulser, Phys. Plasmas 14 (2007) 023301.
[6] S.D. Baton, J.J. Santos, F. Amiranoff, H. Popescu, L. Gremillet, M. Koenig, E. Martinolli, O. Guilbaud, C. Rousseaux, M. Rabec Le Gloahec, T. Hall, D. Batani, E. Perelli, F. Scianitti, T.E. Cowan, Phys. Rev. Lett. 91 (2003) 105001.
[7] A. Macchi, F. Cattani, T.V. Liseykina, F. Cornolti, Phys. Rev. Lett. 94 (2005) 165003.
[8] T.V. Liseikina, A. Macchi, Appl. Phys. Lett. 91 (2007) 171502.
[9] X. Zhang, B. Shen, X. Li, Z. Jin, F. Wang, Phys. Plasmas 14 (2007) 073101.
[10] X. Zhang, B. Shen, X. Li, Z. Jin, F. Wang, M. Wen, Phys. Plasmas 14 (2007) 123108.
[11] A.P.L. Robinson, M. Zepf, S. Kar, R.G. Evans, C. Bellei, New J. Phys. 10 (2008) 013021.
[12] O. Klimo, J. Psikal, J. Limpouch, V.T. Tikhonchuk, Phys. Rev. ST Accel. Beams 11 (2008) 031301.
[13] X.Q. Yan, C. Lin, Z.M. Sheng, Z.Y. Guo, B.C. Liu, Y.R. Lu, J.X. Fang, J.E. Chen, Phys. Rev. Lett. 100 (2008) 135003.
[14] Y. Yin, W. Yu, M.Y. Yu, A. Lei, X. Yang, H. Xu, V.K. Senecha, Phys. Plasmas 15 (2008) 093106.
[15] M. Chen, A. Pukhov, Z.M. Sheng, X.Q. Yan, Phys. Plasmas 15 (2008) 113103.
[16] A.P.L. Robinson, P. Gibbon, M. Zepf, S. Kar, R.G. Evans, C. Bellei, Plasma Phys. Controlled Fusion 51 (2009) 024004.
[17] T.V. Liseikina, D. Prellino, F. Cornolti, A. Macchi, IEEE Trans. Plasma Sci. 36 (2008) 1866.
[18] T.V. Liseikina, M. Borghesi, A. Macchi, S. Tuveri, Plasma Phys. Controlled Fusion 50 (2008) 124033.
[19] F. Cattani, A. Kim, D. Anderson, M. Lisak, Phys. Rev. E 62 (2000) 1234.
[20] D. Prellino, Master's thesis, University of Pisa, Italy, 2007.
[21] A. Macchi, F. Ceccherini, F. Cornolti, S. Kar, M. Borghesi, Plasma Phys. Controlled Fusion 51 (2009) 024005.
[22] S.G. Rykovanov, J. Schreiber, J. Meyer-ter-Vehn, C. Bellei, A. Henig, H.C. Wu, M. Geissler, New J. Phys. 10 (2008) 113005.
[23] V.A. Vshivkov, N.M. Naumova, F. Pegoraro, S.V. Bulanov, Phys. Plasmas 5 (1998) 2727.
[24] F. Pegoraro, S.V. Bulanov, Phys. Rev. Lett. 99 (2007) 065002.
[25] I.V. Sokolov, Sov. Phys. Usp. 34 (1991) 925.
[26] M.G. Haines, Phys. Rev. Lett. 87 (2001) 135005.
[27] C. Thaury, F. Quéré, J.-P. Geindre, A. Levy, T. Ceccotti, P. Monot, M. Bougeard, F. Réau, P. d'Oliveira, P. Audebert, R. Marjoribanks, Ph. Martin, Nat. Phys. 3 (2007) 424.
[28] J. Badziak, S. Glowacz, S. Jablonski, P. Parys, J. Wolowski, H. Hora, J. Krása, L. Láska, K. Rohlena, Plasma Phys. Controlled Fusion 46 (2004) B541.

[29] S. Kar, M. Borghesi, S.V. Bulanov, M.H. Key, T.V. Liseykina, A. Macchi, A.J. Mackinnon, P.K. Patel, L. Romagnani, A. Schiavi, O. Willi, Phys. Rev. Lett. 100 (2008) 225004.
[30] K.U. Akli, S.B. Hansen, A.J. Kemp, R.R. Freeman, F.N. Beg, D.C. Clark, S.D. Chen, D. Hey, S.P. Hatchett, K. Highbarger, E. Giraldez, J.S. Green, G. Gregori, K.L. Lancaster, T. Ma, A.J. MacKinnon, P. Norreys, N. Patel, J. Pasley, C. Shearer, R.B. Stephens, C. Stoeckl, M. Storm, W. Theobald, L.D. Van Woerkom, R. Weber, M.H. Key, Phys. Rev. Lett. 100 (2008) 165002.
[31] L.O. Silva, M. Marti, J.R. Davies, R.A. Fonseca, C. Ren, F.S. Tsung, W.B. Mori, Phys. Rev. Lett. 92 (2004) 015002.